Copy 44
RM SL57K19

NACA

RESEARCH MEMORANDUM

for the

U. S. Air Force

INVESTIGATION OF THE LOW-SPEED FLIGHT CHARACTERISTICS OF A 1/15-SCALE MODEL OF THE CONVAIR XB-58 AIRPLANE

COORD. NO. AF-AM-15

By John W. Paulson

Langley Aeronautical Laboratory
Langley Field, Va. [redacted]

[redacted]

CLASSIFIED DOCUMENT

This material contains information affecting the National Defense of the United States within the meaning of the espionage laws, Title 18, U.S.C., Secs. 793 and 794, the transmission or revelation of which in any manner to an unauthorized person is prohibited by law.

NATIONAL ADVISORY COMMITTEE FOR AERONAUTICS

WASHINGTON

NOV 14 1957

NATIONAL ADVISORY COMMITTEE FOR AERONAUTICS

RESEARCH MEMORANDUM

for the

U. S. Air Force

INVESTIGATION OF THE LOW-SPEED FLIGHT CHARACTERISTICS OF A 1/15-SCALE MODEL OF THE CONVAIR XB-58 AIRPLANE

COORD. NO. AF-AM-15

By John W. Paulson

SUMMARY

An investigation of the low-speed stability and control characteristics of a 1/15-scale free-flying model of the Convair XB-58 airplane has been made in the Langley full-scale tunnel by the Langley free-flight tunnel section. The model was flown over an angle-of-attack range from 9° to 30°, and only relatively low-altitude conditions were simulated.

The longitudinal stability and control characteristics were satisfactory over the angle-of-attack range investigated with the center of gravity at 25 percent of the mean aerodynamic chord. With the center of gravity at 30 percent of the mean aerodynamic chord, the model was very sensitive to gusts and control deflection and was somewhat more difficult to fly. The lateral stability characteristics were satisfactory up to an angle of attack of about 30° where static directional instability caused the model to be directionally divergent. The Dutch roll oscillation was well damped over the angle-of-attack range. Adding artificial damping in roll, yaw, or pitch made the model fly more smoothly, roll damping being much more effective than yaw or pitch damping; but the added damping did not have any noticeable effect on the directional divergence. Pod drops were successfully made at scaled-up weights of 8,000 and 15,000 pounds. The pod separated more cleanly with a canard setting of -15° than with a setting of 0°.

~~CONFIDENTIAL~~

UNCLASSIFIED

INTRODUCTION

An investigation of the low-speed stability and control characteristics of a 1/15-scale free-flying model of the Convair XB-58 airplane has been made at the request of the U. S. Air Force. The XB-58 airplane is a 60° delta-wing bomber powered by four pod-mounted turbojet engines. A large jettisonable pod, which carries the warhead and some fuel, is mounted under the fuselage.

The investigation included flight tests of the composite (pod on) and return-component (pod off) configurations and flight tests to determine the effect of dropping the pod. Power-off and power-on force tests were made to determine the static longitudinal stability and control characteristics of the model. Only power-off tests were made to determine the static lateral stability and control characteristics.

In order to permit a better interpretation of the free-flight tests in terms of the full-scale airplane, a comparison was made between the results of the force tests of the flight-test model at a low Reynolds number and force tests made by the manufacturer at a higher Reynolds number.

SYMBOLS

The longitudinal data are referred to the stability system of axes and the lateral data are referred to the body system of axes. (See fig. 1.) The origin of the axes was located to correspond to a longitudinal center-of-gravity position of 25 percent of the mean aerodynamic chord for both the composite and return-component configurations. The vertical location of the center of gravity was 1.6 and 3.2 percent of the mean aerodynamic chord above the pod parting line for the composite and return-component models, respectively.

S	wing area, sq ft
$\bar{c}$	wing mean aerodynamic chord, ft
V	airspeed, ft/sec
b	wing span, ft
q	dynamic pressure, $\frac{\rho V^2}{2}$, lb/sq ft

ρ	air density, slugs/cu ft
β	angle of sideslip, deg
ψ	angle of yaw, deg
ϕ	angle of bank, deg
α	angle of attack of wing, deg
I_X	moment of inertia about longitudinal body axis, slug-ft^2
I_Y	moment of inertia about lateral body axis, slug-ft^2
I_Z	moment of inertia about normal body axis, slug-ft^2
X_s	longitudinal force, lb
Y	lateral force, lb
Z_s	normal force, lb
F_L	lift force, lb
F_D	drag force, lb
T	thrust, lb
F_Y	side force, lb
M_Y	pitching moment, ft-lb
M_X	rolling moment, ft-lb
M_Z	yawing moment, ft-lb
C_L	lift coefficient, Lift/qS
C_D	drag coefficient, Drag/qS
C_m	pitching-moment coefficient, $M_Y/qS\bar{c}$

C_n yawing-moment coefficient, M_Z/qSb

C_l rolling-moment coefficient, M_X/qSb

C_Y lateral-force coefficient, F_Y/qS

ΔC_n, ΔC_l incremental moments due to a control deflection

$C_{n_\beta} = \frac{\partial C_n}{\partial \beta}$ per degree

$C_{l_\beta} = \frac{\partial C_l}{\partial \beta}$ per degree

$C_{Y_\beta} = \frac{\partial C_Y}{\partial \beta}$ per degree

δ_r rudder deflection, deg

δ_e elevator deflection (elevons deflected together for elevator control), deg

δ_a aileron deflection (elevons deflected differentially for aileron control), deg

APPARATUS AND TESTS

Model

The investigation was made with a 1/15-scale model which was constructed at the Langley Laboratory. A three-view drawing of the model is shown in figure 2 and a photograph of the model flying in the Langley full-scale tunnel is shown in figure 3. Table I gives the mass and dimensional characteristics of the full-scale airplane and the scaled-up mass and dimensional characteristics of the model.

For the flight tests and power-on force tests thrust was provided by compressed air supplied through flexible hoses to nozzles mounted in each nacelle. The amount of thrust could be varied, and the maximum output per nozzle was about 6 to 8 pounds. For the force tests and some of the flight tests, the outboard jets were deflected downward 30° in order to obtain trim conditions similar to those of the airplane. This

deflection was necessary because the center of gravity of the model was too high and also because the model required additional thrust to overcome the drag of the flight cable. The combination of these conditions resulted in a very large thrust moment which was reduced by deflecting the jets. The controls were operated remotely by the pilots by means of flicker-type (full on or off) pneumatic servomechanisms which were actuated by electric solenoids. Maximum control deflections used in the flight tests were $\delta_a = \pm 15^\circ$, $\delta_r = \pm 15^\circ$, and $\delta_e = \pm 13^\circ$. Artificial stabilization in roll was provided by a simple rate-type damper. An air-driven rate gyro was the sensing element, and the signal was fed into a servo-actuator which deflected the ailerons in proportion to the roll rate. There was no manual override in the system so that a signal from the rate gyro reduced the manual aileron deflection and thereby decreased the aileron effectiveness.

For the pod-drop tests the pod and the return component were ballasted so that, when the pod was dropped, the return component had either 3 or 6 percent less static margin than the composite.

Test Equipment and Setup

The force tests were conducted in both the Langley free-flight tunnel and the Langley full-scale tunnel. The model was sting mounted, and the forces and moments were measured about the body axes by using three-component strain-gage balances.

The flight investigation was conducted in the Langley full-scale tunnel with the test setup illustrated in figure 4. In this setup there is an overhead safety cable to prevent the model from crashing. Combined with this cable is another cable composed of plastic hoses and wires which provide the compressed air to the model for thrust and the power for the control actuators, respectively. These cables are attached to the model at about the center-of-gravity location. The pitch pilot, located at the side of the test section, controls the pitching motions of the model. The thrust controller, who is also located at the side of the test section, varies the thrust of the model by remotely controlling the air flow to the model through a valve located at the top of the entrance cone. The thrust controller and pitch pilot must coordinate their efforts in order to maintain steady flight. Another operator adjusts the safety cable so as to keep it slack during flight and takes up the slack to prevent the model from crashing if it goes out of control. A second pilot who controls the rolling and yawing motions of the model is located near the bottom of the exit cone. Motion-picture records of the flights are obtained with cameras located at the side of the test section and at the top and bottom of the exit cone.

The flight-test technique employed with this setup is explained by describing a typical flight: A flight is started with the model being towed by the safety cable. When the tunnel speed reaches the flying speed of the model, the model thrust is increased until the flight cable becomes slack. Adjustments to the elevator and thrust are then made, if necessary, to trim the model for the particular airspeed. The flight is then continued to higher or lower airspeeds by changing the trim setting of the elevator and making the necessary adjustments to tunnel speed and model thrust to maintain steady flight.

For the pod-drop tests the same techniques were used, but a separate safety cable was attached to the pod in order to catch it after each drop.

STATIC STABILITY AND CONTROL CHARACTERISTICS OF FLIGHT-TEST MODEL

Longitudinal Stability and Control

Force tests were made in the Langley free-flight tunnel to determine the static longitudinal stability and control characteristics of the composite and the return-component models over an angle-of-attack range from 3° to 39° with power off for elevator deflections of 0° and -10°. These tests were run at a dynamic pressure of 4.71 pounds per square foot, which corresponds to an airspeed of about 63 feet per second at standard sea-level conditions and to a test Reynolds number of 970,000 based on the mean aerodynamic chord of 2.41 feet. Force tests were also made on the return-component model in the Langley full-scale tunnel with power off and on and with elevator settings of 0°, -5°, and -10°. These tests were made with total-thrust values of 0, 3, 8.5, and 17 pounds. The tests were conducted at a dynamic pressure of 5.43 pounds per square foot, which corresponds to an airspeed of about 68 feet per second at standard sea-level conditions and to a test Reynolds number of 1,040,000 based on the mean aerodynamic chord of 2.41 feet.

Presented for comparison with the power-off data are unpublished data for a higher Reynolds number (3,260,000) obtained from tests conducted by the manufacturer. The longitudinal data for both the free-flight and the manufacturer's models are presented for a center-of-gravity position of 25.0 percent of the mean aerodynamic chord.

Presented in figure 5 is a comparison between the free-flight tunnel data and the manufacturer's data for the return-component configuration. These data show that there is fairly good agreement between the

lift-curve slopes and elevator effectiveness of the two models but indicate a slightly higher static margin $\frac{dC_m}{dC_L}$ for the manufacturer's model over part of the angle-of-attack range. The longitudinal characteristics of the free-flight and the manufacturer's composite models are presented in figure 6. The longitudinal characteristics of the free-flight return-component model are also given in figure 6 for comparison purposes. These data show generally good agreement between the characteristics of the free-flight and the manufacturer's models, although the manufacturer's model had more static margin over part of the angle-of-attack range. The free-flight model data show that the pod reduced the longitudinal stability over the angle-of-attack range.

Presented in figure 7 are the longitudinal characteristics of the return-component model for thrust values of 0, 3, 8.5, and 17 pounds with an elevator setting of 0°. These data show a very large increase in lift coefficient with increase in thrust. Approximately 60 percent of this increase can be accounted for by the vertical component of the thrust. The remainder of the lift increase is attributed to induced lift associated with the action of the compressed-air jets on the wing. These data also show that the static longitudinal stability increased slightly as the thrust increased.

The data of figure 8 show the longitudinal characteristics of the return component with elevator deflections of 0°, -5°, and -10° for each thrust condition tested. From these data it is seen that the elevator effectiveness was virtually unaffected by increasing thrust.

Lateral Stability and Control

Force tests were made to determine the static lateral stability and control characteristics of the composite and return-component models over a sideslip range up to ±20° and for angles of attack from 3° to 39°. These data were obtained in the Langley free-flight tunnel at the same dynamic pressure and center-of-gravity location as the longitudinal data.

The lateral stability characteristics of the free-flight-tunnel composite and return-component models are presented in figures 9 and 10, respectively. The data of figures 9 and 10 are summarized in figure 11 in terms of the side-force parameter C_{Y_β}, the directional-stability parameter C_{n_β}, and the effective-dihedral parameter $-C_{l_\beta}$. These data are presented for sideslip angles of ±5°. Presented for comparison with the free-flight tunnel data are unpublished data for a higher Reynolds number (3,260,000) obtained from tests conducted by the manufacturer.

The directional stability of both the composite model and the return-component model was approximately constant up to an angle of attack of 24° and then dropped rapidly to large negative values. The return-component model had somewhat greater directional stability at all angles of attack and became unstable at a slightly higher angle of attack. The positive effective dihedral of both configurations increased up to about 24° and then decreased rapidly to a negative value. The lateral characteristics of the free-flight model were in good agreement with the higher scale manufacturer's data over their common angle-of-attack range.

The control effectiveness of the free-flight and the manufacturer's return-component models is compared in figures 12 and 13 for the ailerons and rudder, respectively. These data show that the rolling moments produced by the ailerons are in fairly good agreement for the two models but the free-flight model had somewhat less yawing due to aileron deflection. The yawing moments produced by the rudder are in fairly good agreement, but the rolling moments produced by the rudder are smaller for the free-flight model.

FLIGHT TESTS

Flight tests were made to study the stability and control characteristics of the model over an angle-of-attack range from 9° to 30°. The stability and control characteristics of the composite configuration were studied with coordinated ailerons and rudder and with ailerons alone. These tests included flights to determine the effect of adding artificial damping in roll, yaw, or pitch. The control characteristics of the return component were compared with ailerons alone and with rudder used either with or against the ailerons. This control study was made to investigate an emergency condition which might arise because of the failure of certain components of the power control equipment. In some cases this condition would result in adverse rudder being applied with aileron control. Flights were also made to study the effect of dropping the pod.

The pod-drop tests and the return-component control tests were made with the outboard jets deflected down 30° to obtain trim conditions similar to those of the airplane as pointed out previously. The jets were not deflected during the composite-model tests; thus, down-elevator deflection was needed to trim the model at high angles of attack and high thrust conditions. Maximum control deflections used in the flight tests were $\delta_a = \pm 15°$, $\delta_r = \pm 15°$, and $\delta_e = \pm 13°$. Only relatively low altitude conditions were simulated.

The model behavior during flight was observed by the pitch pilot located at the side of the test section and by the roll and yaw pilot

located in the rear of the test section. The results obtained were based on pilot's observations and data obtained from motion-picture records.

FLIGHT TEST RESULTS AND DISCUSSION

A motion-picture film supplement covering flight tests of the model has been prepared and is available on loan. A request card form and a description of the film will be found at the back of this paper on the page immediately preceding the abstract and index page.

Interpretation of Flight-Test Results

The mass data presented in table I show that the model had values of the scaled-up moments of inertia generally similar to those of the full-scale airplane. It has been shown that the static stability characteristics of the low Reynolds number free-flight model are in fairly good agreement with higher Reynolds number results of the manufacturer's model. It is likely, however, that the changes noted in the stability derivatives at high angles of attack will occur at somewhat higher angles of attack for the airplane than for the model. The dynamic behavior of the airplane is therefore expected to be similar to that of the free-flight model except that corresponding dynamic behavior might occur at higher angles of attack.

Longitudinal Stability and Control

Basic model.- The longitudinal stability and control characteristics of both the composite and return-component models were satisfactory over the angle-of-attack range flown with the center of gravity at 25 percent of the mean aerodynamic chord. The models were longitudinally steady and response to control was good. With the center of gravity moved rearward to about 30 percent of the mean aerodynamic chord, the model became much more sensitive to elevator deflections and to gusts and thus was more difficult to control. Flights could be maintained, however, with careful attention to control.

Pitch damping added.- Adding artificial damping in pitch with the center of gravity at either $0.25\bar{c}$ or $0.30\bar{c}$ slowed down the pitching motions and enabled the pitch pilot and thrust controller to coordinate their controls better and smoother flights resulted.

Lateral Stability and Control

Basic model.- The lateral (Dutch roll) oscillation of the composite and return-component configurations were well damped at all angles of attack. The directional stability characteristics of the model were generally satisfactory over the angle-of-attack range investigated except near the stall. As the model approached an angle of attack of 30°, there was an increasing tendency of the model to diverge in sideslip, but the pilot could usually maintain flight by careful attention to control. When the angle of attack reached 30°, the model could no longer be kept under control and it experienced a directional divergence. The divergence can be explained by the static directional stability data of figures 9 to 11. As the angle of attack increases, the static directional stability decreases and the sideslip range over which the model is directionally stable also decreases. Another factor which might have contributed to the directional divergence is the decrease in positive effective dihedral at the higher angles of attack.

The lateral control characteristics of both configurations were considered to be satisfactory with coordinated ailerons and rudder over the angle-of-attack range investigated. There was no evidence of any appreciable decrease in control effectiveness as the angle of attack increased and the model was controlled satisfactorily up to the angle of attack at which it diverged. The control was also generally satisfactory with ailerons alone unless the model was badly disturbed, in which case recovery from the disturbance was usually difficult. It was also found that coordinated ailerons and rudder provided better control at high angles of attack where the model began to yaw due to the loss in directional stability.

Yaw damping added.- The general flight behavior of the model was not appreciably changed by adding yaw damping although the model did appear to be a little steadier in yaw, particularly at angles of attack approaching 30°. The model still experienced a directional divergence, however, and the divergence appeared to be more abrupt than that of the basic model. This behavior was probably a result of the increased steadiness in yaw up to the angle of attack at which the model diverged.

Roll damping added.- Increasing the roll damping greatly improved the overall flight behavior of the model. The increase in damping eliminated the abrupt motions associated with the flicker-type control or those caused by gust disturbances and resulted in smooth, steady flights. The added damping greatly increased the stiffness in roll and reduced the maneuverability, but the model was easy to fly and required very little attention to control. There was no apparent effect of the added roll damping on the directional divergence.

Yaw and roll damping added.- With both yaw and roll damping added, the behavior of the model was essentially the same as it was with only roll damping added. The yawing motions were reduced as they were when yaw damping alone was added, but the biggest improvement in the model characteristics resulted from the increase in the roll damping. The added damping in roll and yaw did not have any noticeable effect on the directional divergence.

Yaw, roll, and pitch damping added.- Increasing the damping about all three axes resulted in very smooth and steady flights. The model virtually flew itself and only an occasional control application was required on the part of the pilot to keep the model from drifting sideways in the test section. The model again lacked maneuverability mainly because of its stiffness in roll and it still experienced a directional divergence at an angle of attack of 30°.

Effect of rudder on lateral control characteristics.- For the control tests made to compare the lateral control characteristics of the model with ailerons alone and with rudder used either with or against the ailerons, the aileron deflection was held constant at ±7° while rudder deflections of ±7° and ±15° were used to give ratios of δ_r/δ_a of 1 and 2. No artificial damping was used in these tests.

The flight tests of the return component at an angle of attack of 9° indicated that satisfactory control was obtained with ailerons alone as long as the model was not badly disturbed. After a disturbance it was difficult to settle the model down. When the rudder was used with the ailerons and $\delta_r/\delta_a = 1$, the model had very good control characteristics, but, when a ratio of $\delta_r/\delta_a = 2$ was used, it was found that the rudder deflection was too large and excessive yawing motions of the model resulted.

When the rudder was used against the ailerons, flights were very difficult to perform. With $\delta_r/\delta_a = 1$, constant attention to control was required, but the model could be kept under control. Typical of these flights were large sidewise displacements that the model sometimes experienced when it became disturbed and efforts were made to steady it. These displacements were much worse with $\delta_r/\delta_a = 2$ and the flights generally terminated with the model going out of control.

The flight tests of the composite model at an angle of attack of 15° showed that the control characteristics were generally similar to those of the return-component model. In this condition, when the rudder was used against the ailerons and the value of δ_r/δ_a was 2, the model went out of control at the moment of rudder reversal.

Pod-Drop Investigation

Some preliminary flights were made to determine the effect of the pitch damper on the behavior of the model at pod drop. These flights indicated that the damper had relatively little effect on the model behavior; thus all further tests were made with pitch damping added as well as roll damping in order to obtain as steady a flying condition as possible for the drops.

Effect of pod weight.- The investigation showed that the pod with the canard set at 0° could be dropped at scaled-up weights of 8,000 pounds or 15,000 pounds (with a return component at 95,000 pounds) without introducing any violent uncontrollable motions due to the abrupt trim change. Although the static margin $-\frac{dC_m}{dC_L}$ changed from 0.09 for the composite model to 0.03 for the return-component model when the 15,000-pound pod was dropped and from 0.06 to 0.03 when the 8,000-pound pod was dropped, the return-component model could be easily controlled after the drop by proper coordination of elevator and thrust control. Down elevator was applied at the moment the pod was dropped to balance out the change in trim caused by the rearward movement of the center of gravity and the thrust was reduced so that the return-component model did not climb.

It appeared during these flights that the heavy pod broke away from the return-component model more cleanly then did the light pod. This result was probably due to the fact that the speed and angle of attack at the time of drop were approximately those required to fly the light pod but were not sufficient to fly the heavy pod.

With the canard surface set at 0° incidence, the pod sometimes did not break cleanly away from the return-component model. This was especially true for the light pod which generally dropped free without much change in pitch attitude and moved back while still relatively close to the return-component model. At no time, however, did the pod strike the return-component model.

Effect of canard deflection.- When the canard surface was set at -15°, the pod cleared the return-component model more positively than it did with the canard surface set at 0° because upon being released the pod immediately pitched down and rotated to large negative angles of attack as it dropped away from the return-component model.

Effect of sideslip and pod directional stability.- Several drops were made with the light pod in an effort to determine whether the behavior of the pod at drop was influenced by sideslip or by removing the pod lower vertical tail. The drops were made with the model sideslipping

about 5° and with the canard at 0° and -15° deflection. These tests showed that removing the vertical tail from the pod or flying the model in a sideslipped attitude had no noticeable effect on the drop characteristics of the pod.

CONCLUSIONS

Results have been presented from a free-flight stability and control investigation of a 1/15-scale model of the Convair XB-58 airplane. The model was flown over an angle-of-attack range from 9° to 30° and only relatively low-altitude conditions were simulated. From the results, the following conclusions were drawn:

1. The longitudinal stability and control characteristics were satisfactory over the angle-of-attack range investigated with the center of gravity at the 0.25 mean aerodynamic chord. With the center of gravity at the 0.30 mean aerodynamic chord the model was very sensitive to gusts and control deflection and thus was more difficult to fly.

2. The lateral stability characteristics were satisfactory up to an angle of attack of about 30° where static directional instability caused the model to be directionally divergent. The Dutch roll oscillation was well damped over the angle-of-attack range.

3. Adding artificial damping in roll, yaw, or pitch made the model fly more smoothly, roll damping being much more effective than yaw and pitch damping. Artificial damping did not have any noticeable effect on the directional divergence.

4. Pod drops were successfully made at scaled-up weights of 8,000 and 15,000 pounds. The pod separated more cleanly with a canard setting of -15° than with a setting of 0°.

Langley Aeronautical Laboratory,
National Advisory Committee for Aeronautics,
Langley Field, Va., Oct. 25, 1957.

TABLE I.- MASS AND DIMENSIONAL CHARACTERISTICS OF THE CONVAIR XB-58 AIRPLANE AND SCALED-UP CHARACTERISTICS OF THE 1/15-SCALE FREE-FLIGHT MODEL

(a) Mass characteristics

	Scaled-up model		Full-scale airplane	
	Composite	Return component	Composite	Return component
Weight for -				
General flight tests, lb	112,000	---	147,000	---
Control tests, lb	---	64,000	---	---
Pod-drop tests (heavy pod), lb	110,800	95,600	110,000	95,000
Pod-drop tests (light pod), lb	103,700	95,600	110,000	102,000
Moments of inertia for -				
General flight tests:				
I_X, slug-ft^2	387,000	---	398,000	---
I_Y, slug-ft^2	1,085,000	---	1,072,000	---
I_Z, slug-ft^2	1,420,000	---	1,413,000	---
Control tests:				
I_X, slug-ft^2	388,000	380,000	307,000	296,000
I_Y, slug-ft^2	1,162,000	1,050,000	748,000	567,000
I_Z, slug-ft^2	1,490,000	1,375,000	1,015,000	867,000
Pod-drop tests (heavy pod):				
I_X, slug-ft^2	350,000	342,000	382,000	363,000
I_Y, slug-ft^2	920,000	783,000	936,000	732,000
I_Z, slug-ft^2	1,262,000	1,125,000	1,252,000	1,027,000
Pod-drop tests (light pod):				
I_X, slug-ft^2	350,000	342,000	382,000	370,000
I_Y, slug-ft^2	875,000	783,000	936,000	771,000
I_Z, slug-ft	1,216,000	1,125,000	1,252,000	1,090,000
Moment of inertia about lateral axis for heavy pod, I_Y, slug-ft^2	46,300		44,500	
Moment of inertia about lateral axis for light pod, I_Y, slug-ft^2	35,300		35,000	

TABLE I.- MASS AND DIMENSIONAL CHARACTERISTICS OF THE CONVAIR XB-58 AIRPLANE AND SCALED-UP CHARACTERISTICS OF THE 1/15-SCALE FREE-FLIGHT MODEL - Continued

(b) Dimensional characteristics of full-scale return component

Wing:	
Airfoil section:	
Root chord	NACA 0003.46-64.069
Span station 3.767 and outboard	NACA 0004.08-63
Area (total), sq ft	1543
Span, ft	56.9
Aspect ratio	2.1
Root chord, ft	54.2
Tip chord, ft	0
Mean aerodynamic chord, ft	36.2
Sweepback of leading edge, deg	60
Sweepforward of trailing edge, deg	10
Dihedral, deg	0
Incidence, deg	3
Elevons:	
Area behind hinge line (two surfaces), sq ft	211
Span (two surfaces), ft	37
Root chord, ft	7.2
Tip chord, ft	4.1
Vertical tail:	
Airfoil section	NACA 0005-64
Area (exposed), sq ft	1257
Span, ft	13.23
Aspect ratio	1.4
Root chord, ft	13.5
Tip chord, ft	5.4
Sweepback of leading edge, deg	50
Sweepback of trailing edge, deg	30
Rudder:	
Area behind hinge line, sq ft	25.4
Span, ft	9.7
Root chord, ft	2.8
Tip chord, ft	2.4

TABLE I.- MASS AND DIMENSIONAL CHARACTERISTICS OF THE CONVAIR XB-58 AIRPLANE AND SCALED-UP CHARACTERISTICS OF THE 1/15-SCALE FREE-FLIGHT MODEL - Concluded

(c) Dimensional characteristics of full-scale pod

Wing:	
Airfoil section	NACA 0004.5-64
Area (total), sq ft	140
Span, ft	17.1
Aspect ratio	2.1
Root chord, ft	16.4
Tip chord, ft	0
Mean aerodynamic chord, ft	10.9
Sweepback of leading edge, deg	60
Sweepforward of trailing edge, deg	10
Dihedral, deg	0
Incidence, deg	0
Canard:	
Airfoil section	NACA 0004.5-64
Area (total), sq ft	46
Span, ft	9.8
Aspect ratio	2.1
Root chord, ft	9.4
Tip chord, ft	0
Mean aerodynamic chord, ft	6.2
Sweepback of leading edge, ft	60
Sweepforward of trailing edge, ft	10
Dihedral, deg	0
Incidence, deg	0, -15
Ventral fin:	
Airfoil section	NACA 0004.5-64
Area (exposed), sq ft	21.7
Span, ft	5.1
Aspect ratio	1.75
Root chord, ft	8.7
Tip chord, ft	3
Sweepback of leading edge, deg	60

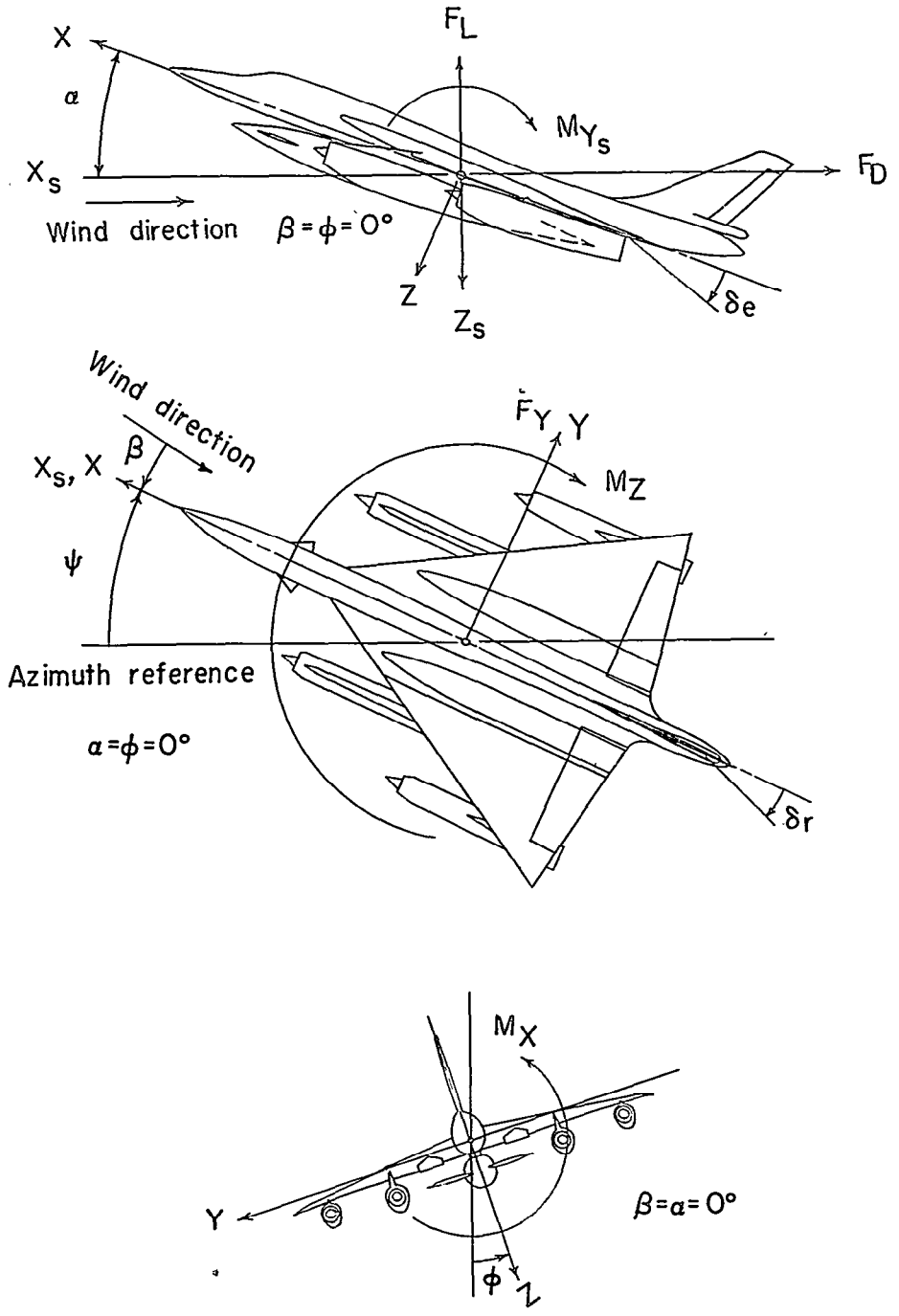

Figure 1.- System of axes used in investigation. Longitudinal data are referred to stability system of axes, and lateral data are referred to body system of axes. Arrows indicate positive directions of moments, forces, and angles.

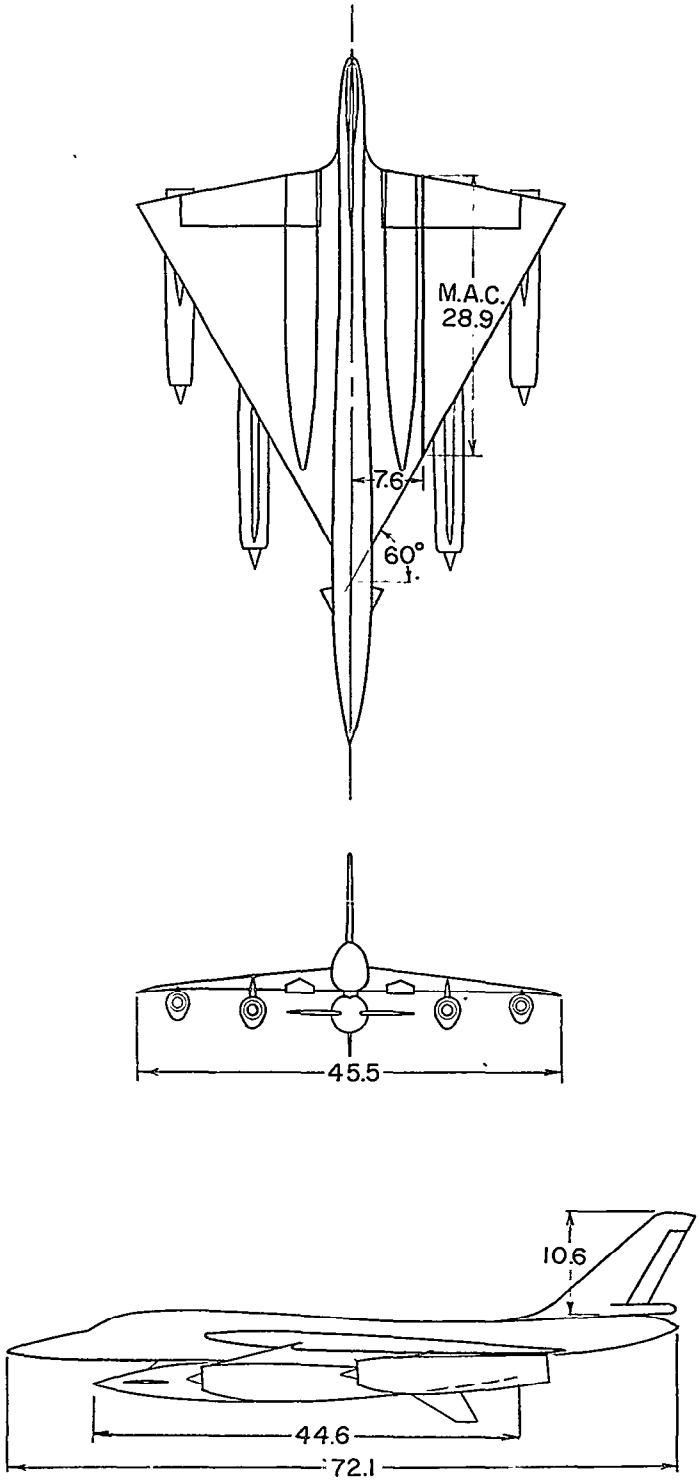

Figure 2.- Three-view drawing of 1/15-scale model of Convair XB-58 airplane used in investigation. All dimensions are in inches.

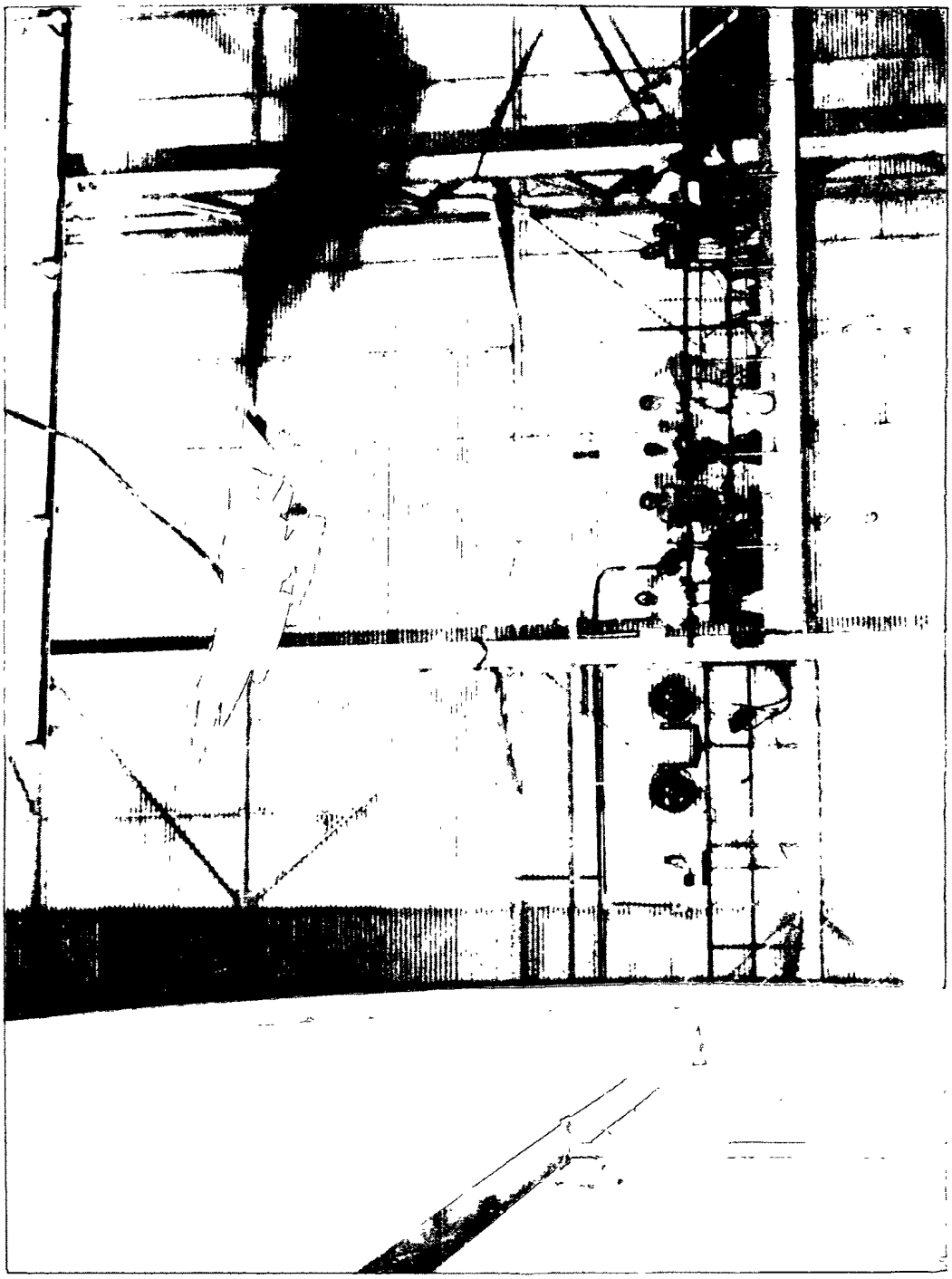

L-96279

Figure 3.- Model flying in Langley full-scale tunnel.

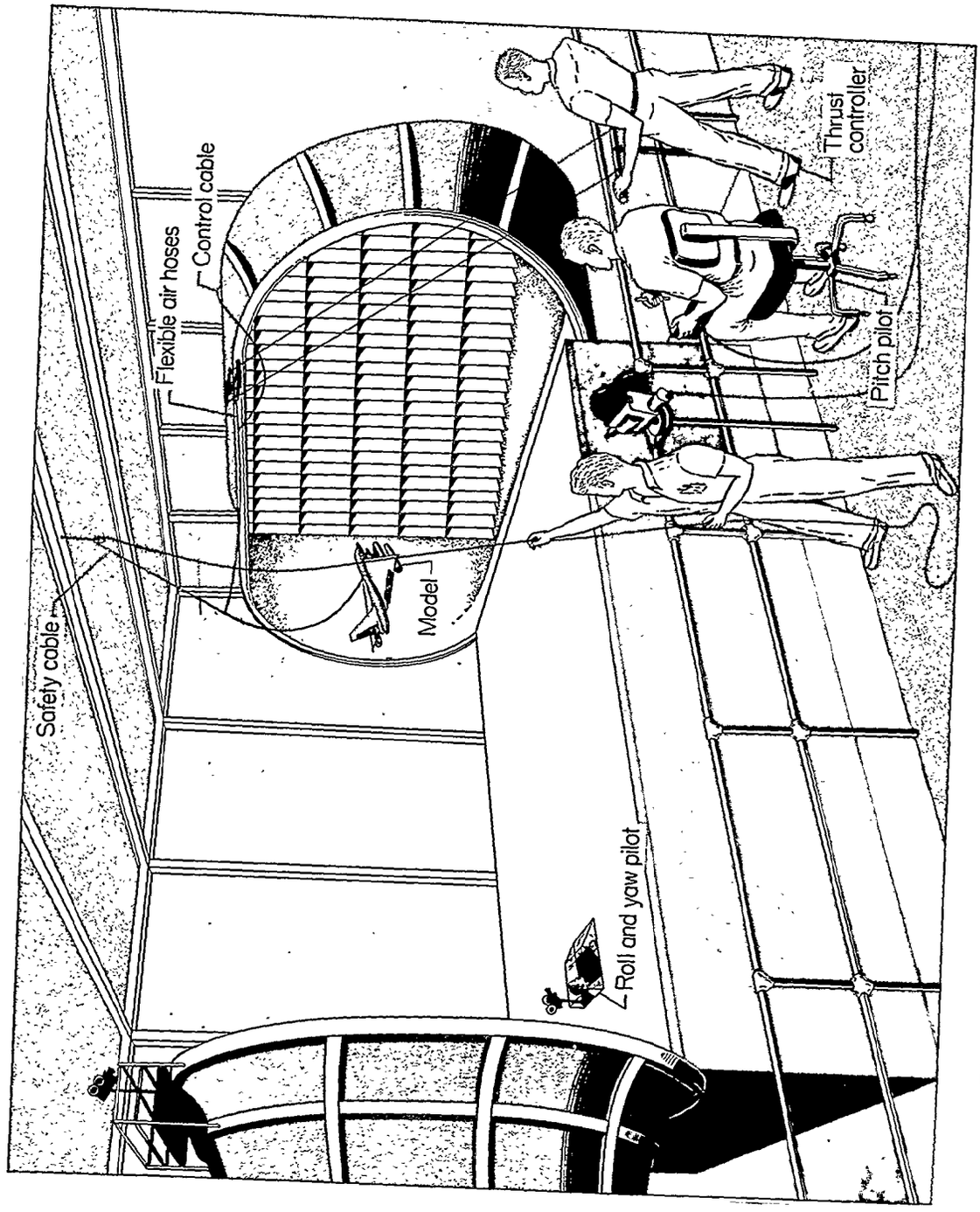

Figure 4.- Sketch of test setup in Langley full-scale tunnel.

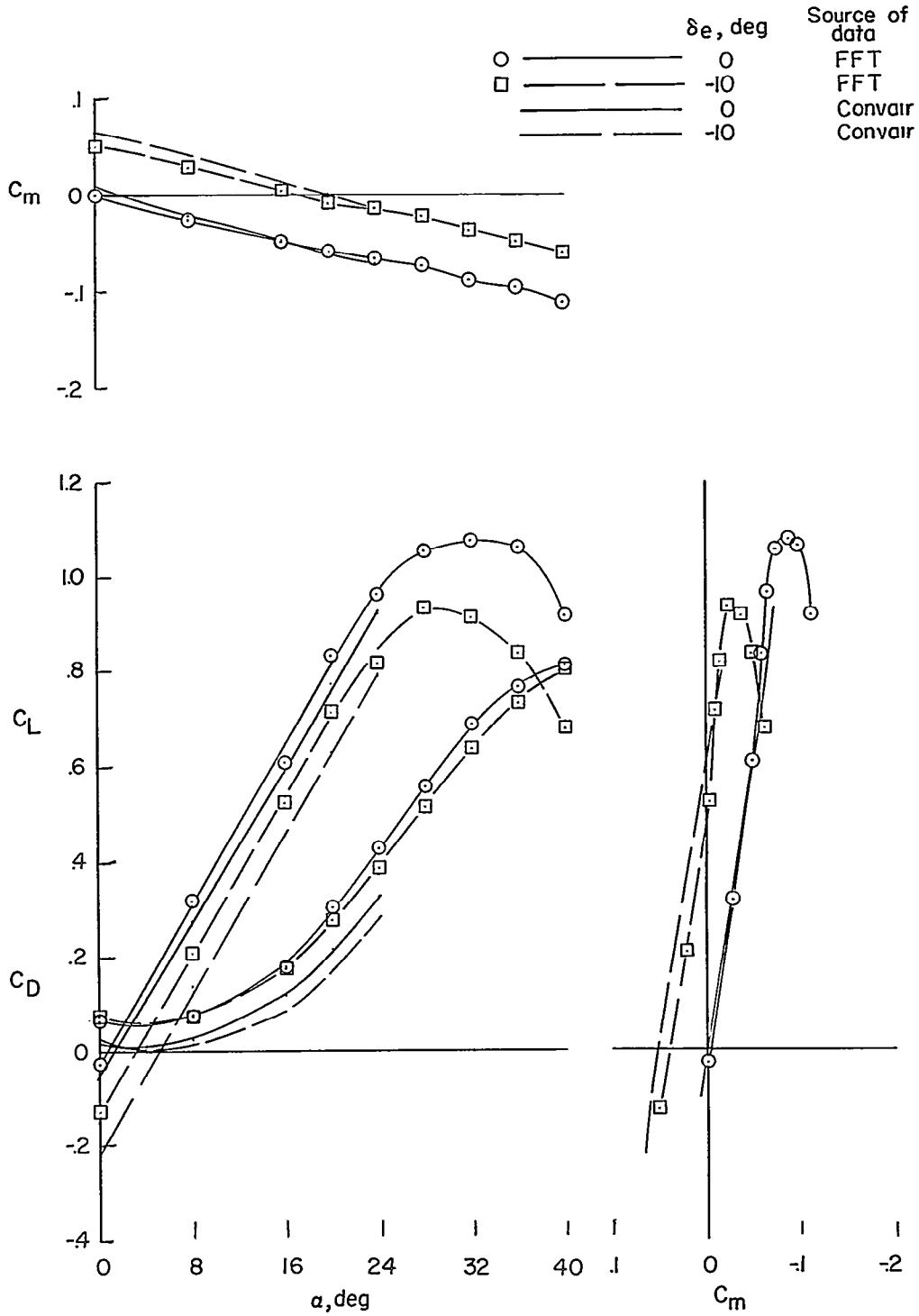

Figure 5.- Aerodynamic characteristics of free-flight and Convair return-component models. $\beta = 0^{\circ}$.

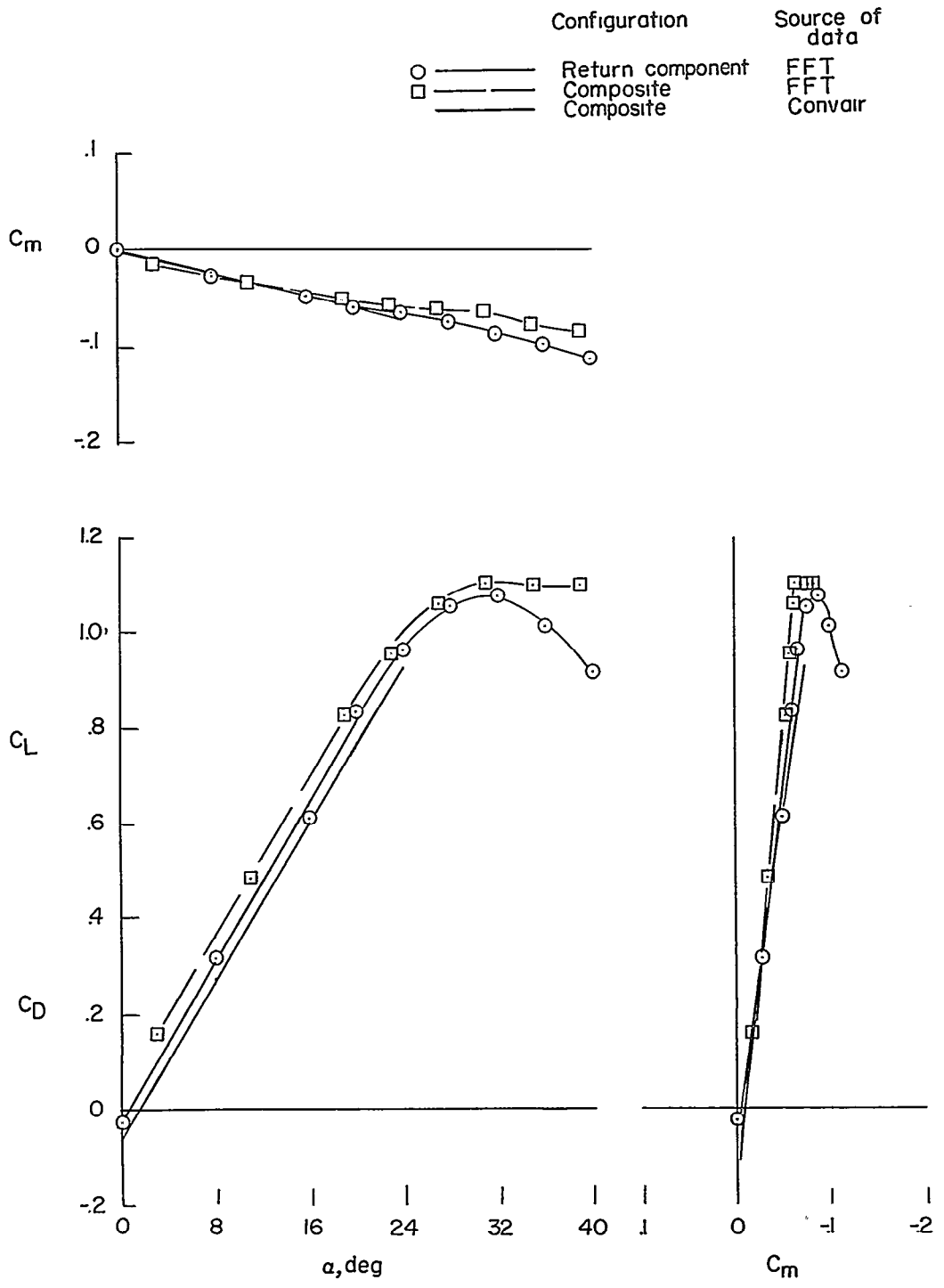

Figure 6.- Aerodynamic characteristics of free-flight composite and return-component models and Convair composite model. $\beta = 0^{\circ}$.

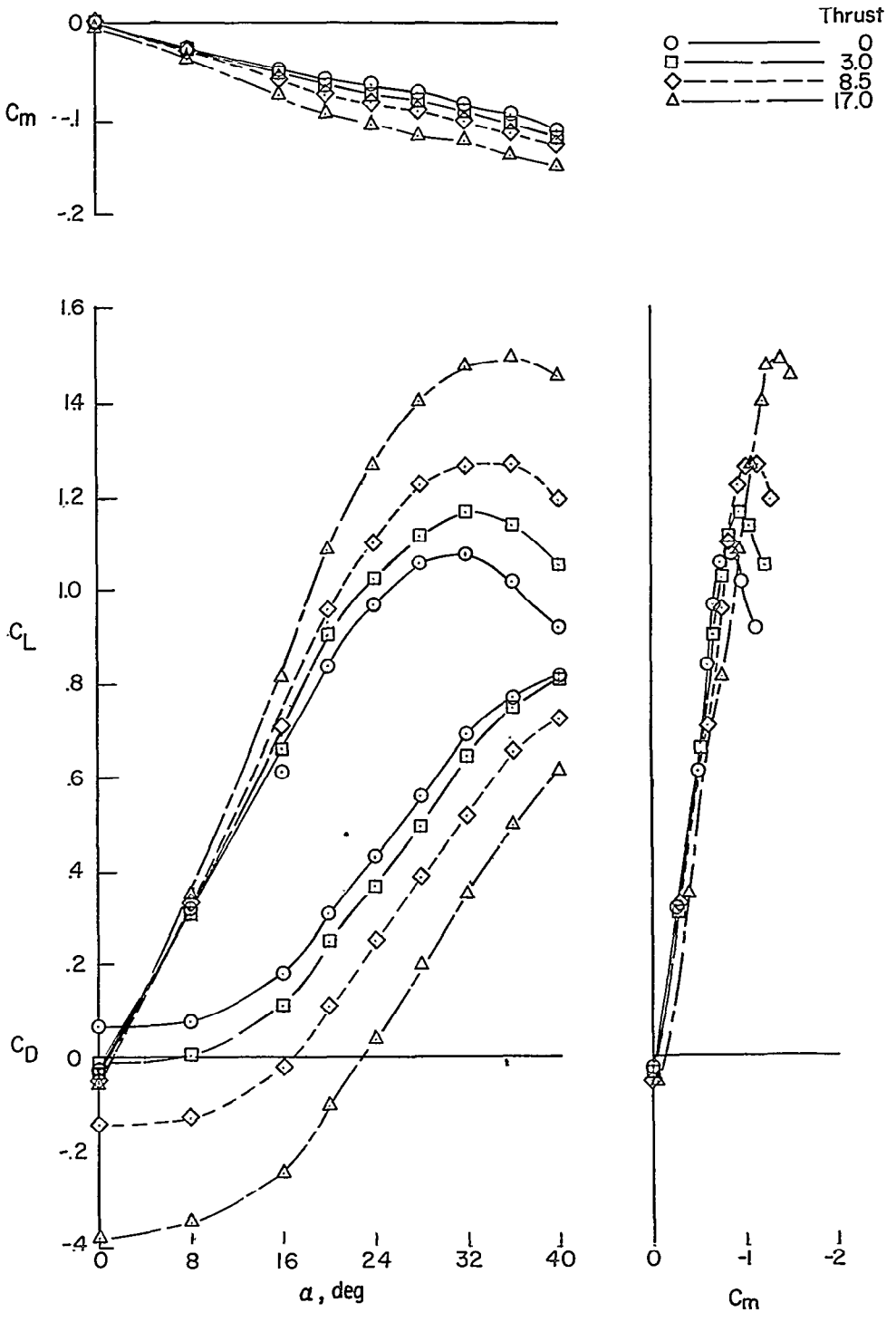

Figure 7.- Effect of thrust on aerodynamic characteristic of free-flight return-component model. $\beta = 0^{\circ}$; $\delta_e = 0^{\circ}$.

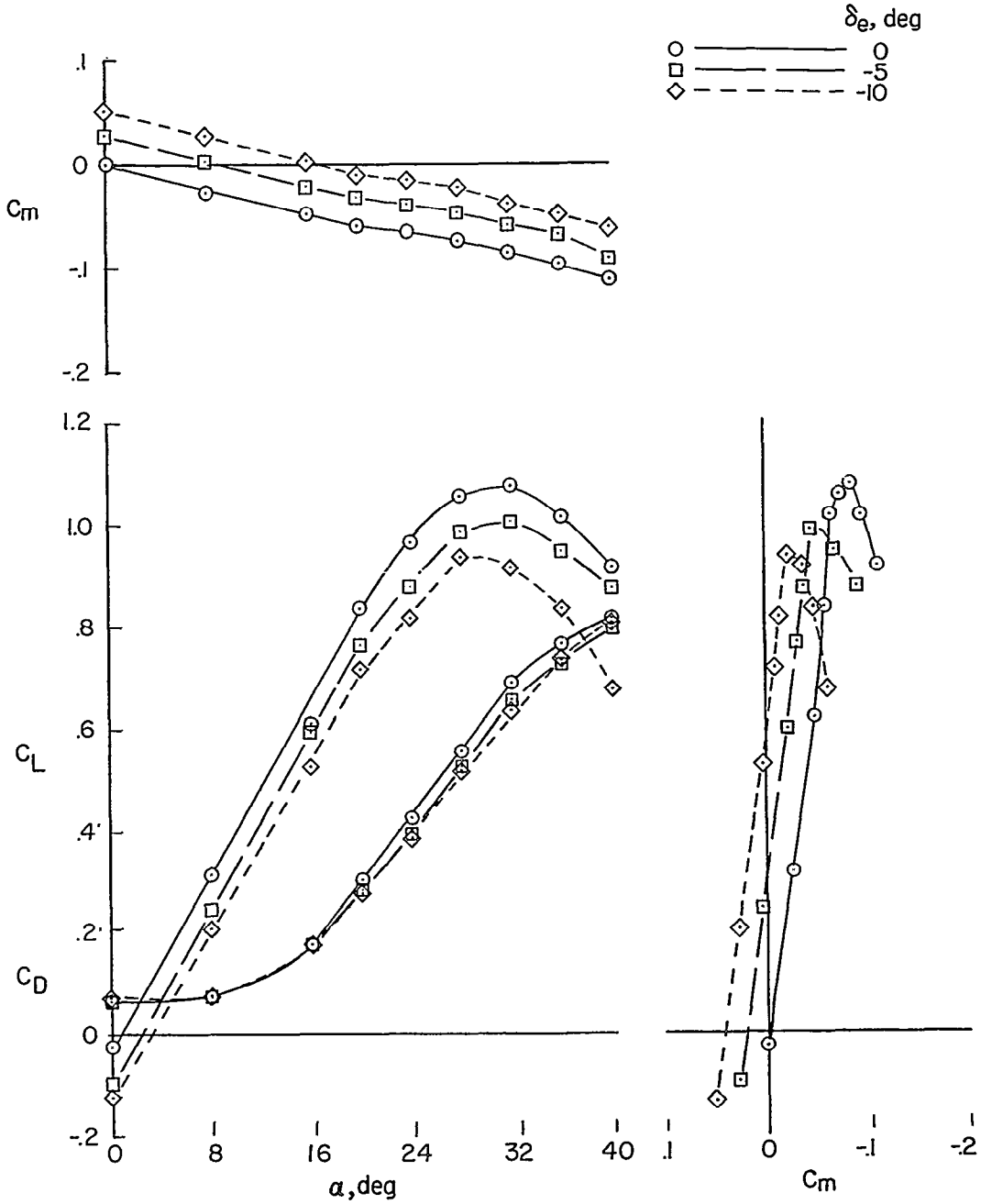

(a) T = 0 lbs.

Figure 8.- Effect of elevator deflection on aerodynamic characteristics of free-flight return-component model for various thrust settings. $\beta = 0^{\circ}$.

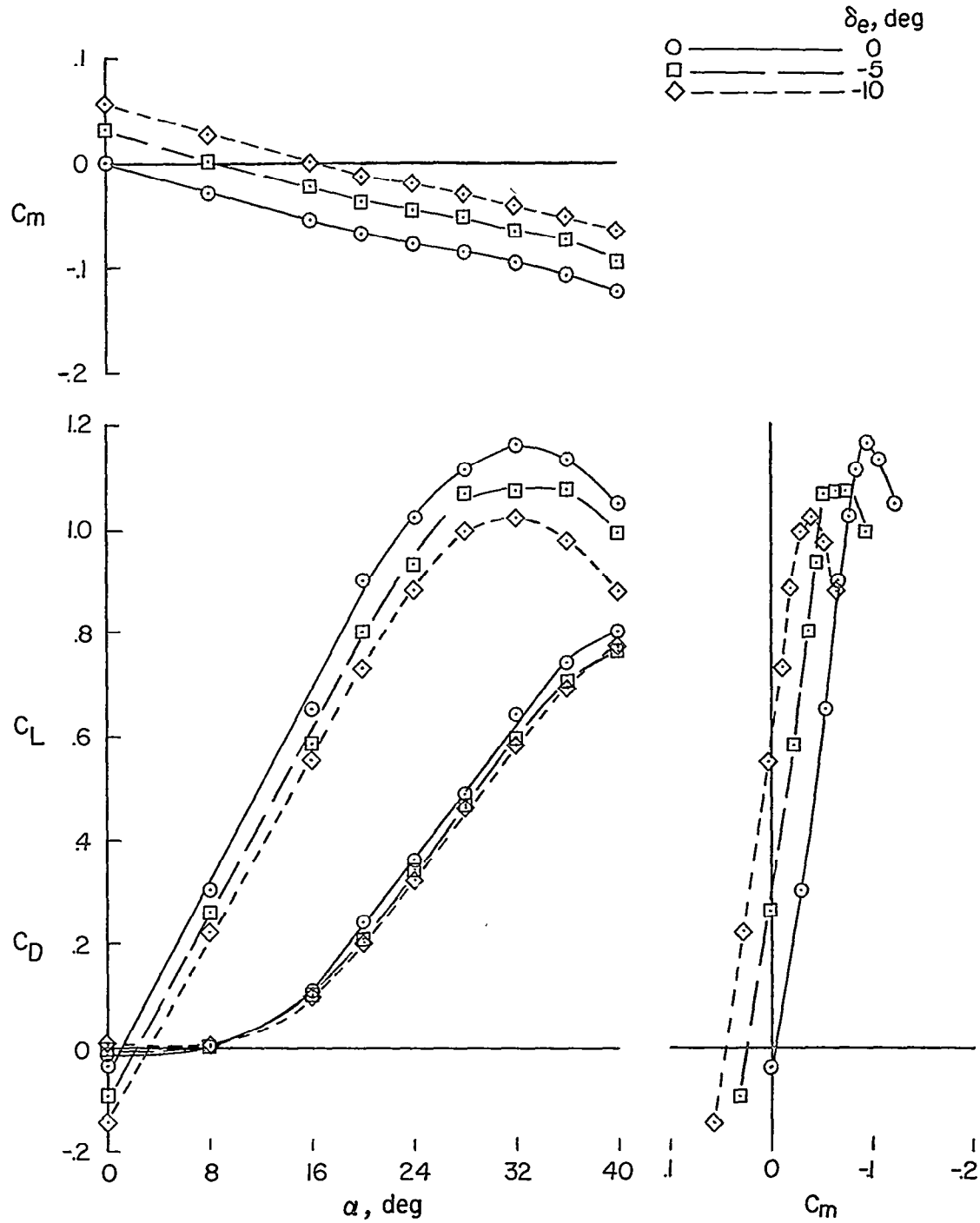

(b) T = 3.0 lbs.

Figure 8.- Continued.

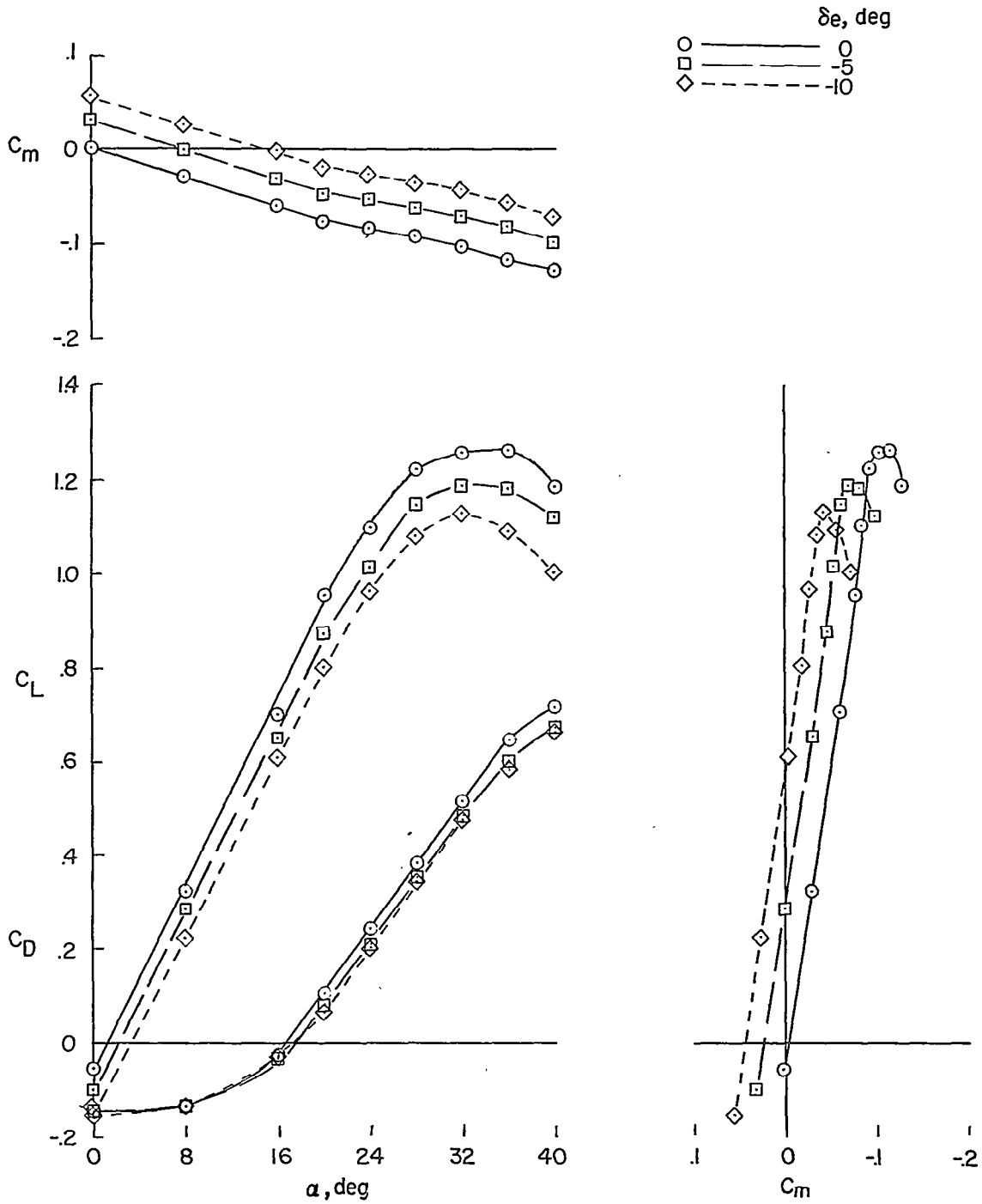

(c) T = 8.5 lbs.

Figure 8.- Continued.

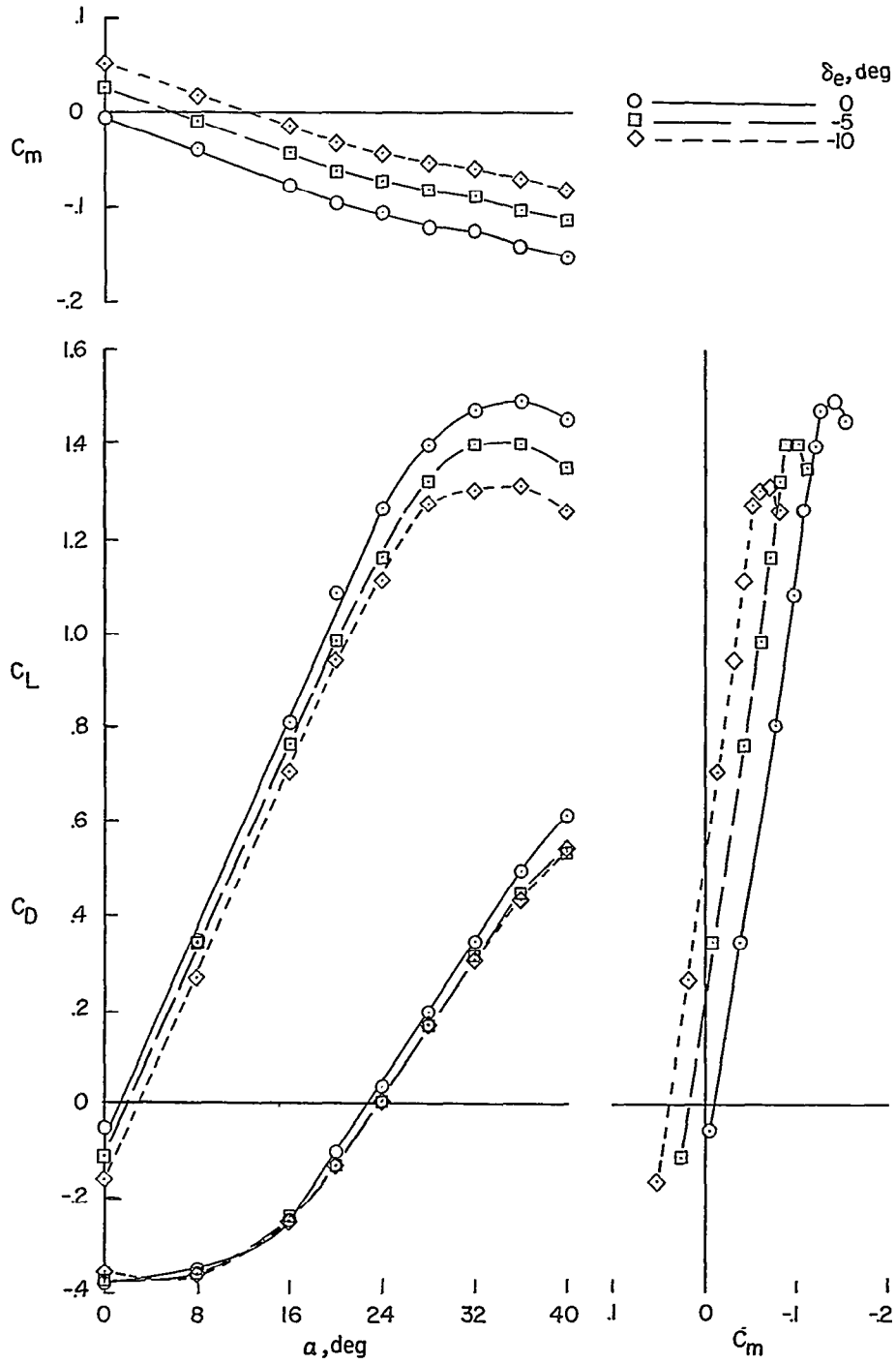

(d) T = 17.0 lbs.

Figure 8.- Concluded.

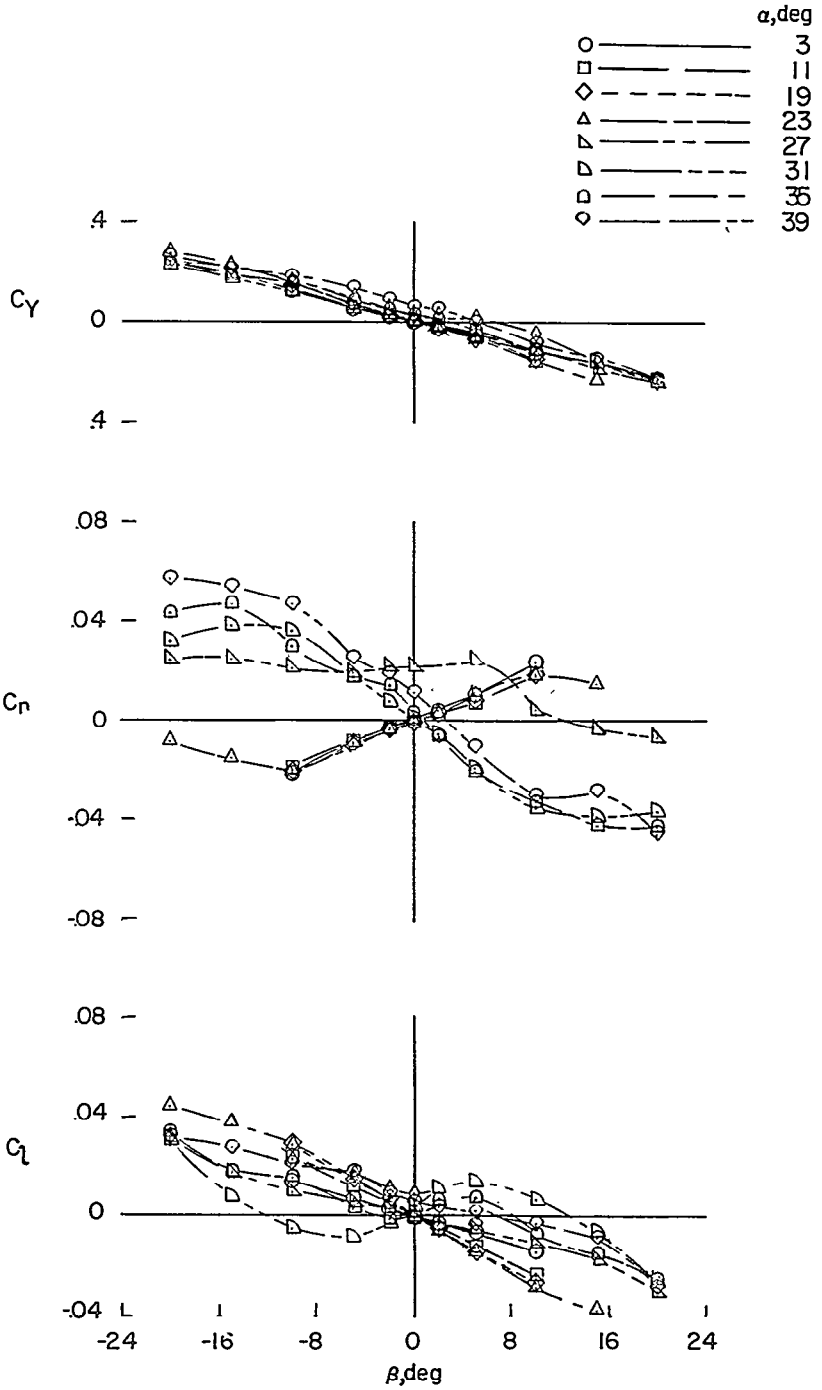

Figure 9.- Variation of static lateral stability characteristics of free-flight model with angle of sideslip. Composite model; $\delta_e = 0^\circ$; T = 0 lbs.

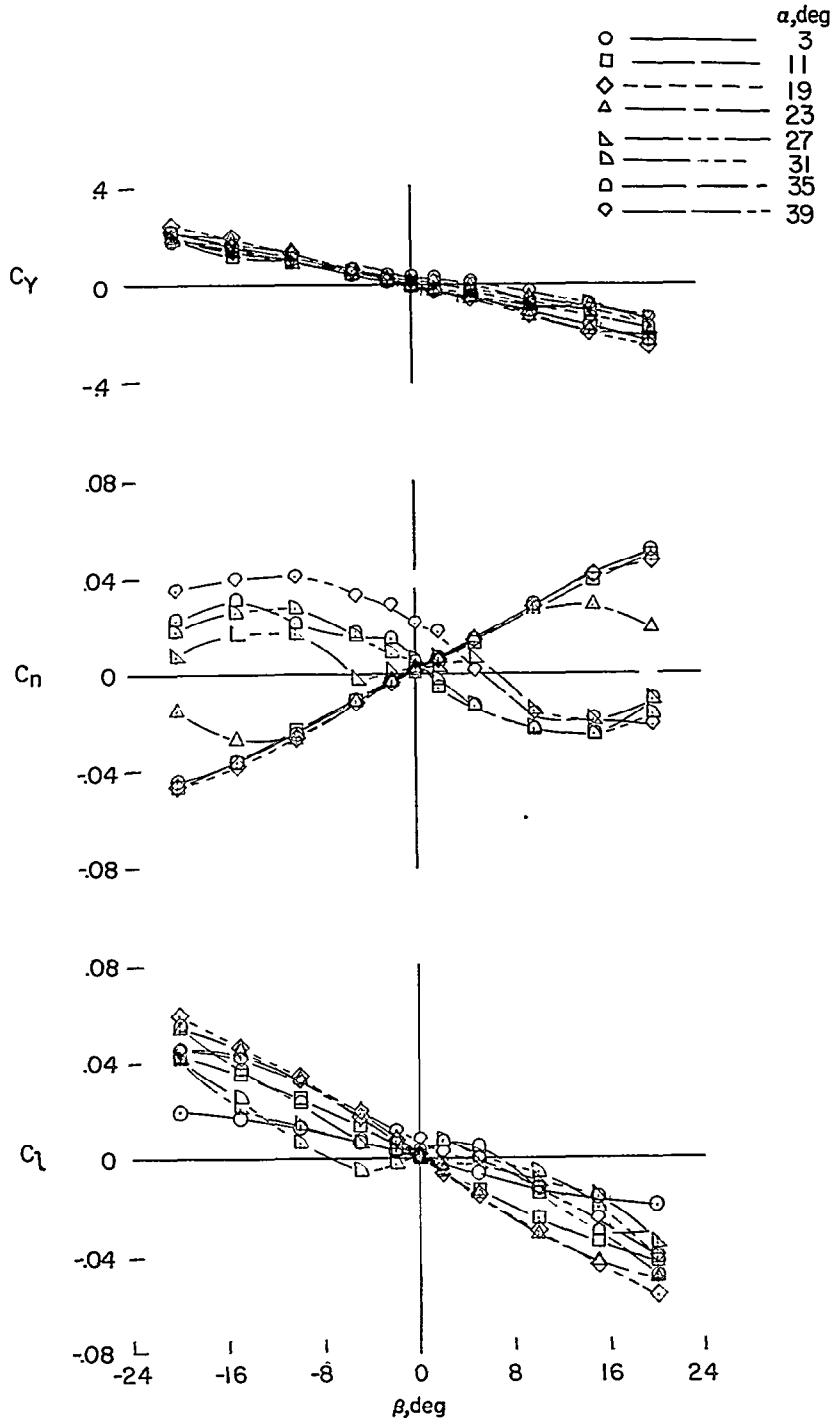

Figure 10.- Variation of static lateral stability characteristics of free-flight model with angle of sideslip. Return-component model; $\delta_e = 0^o$; T = 0 lbs.

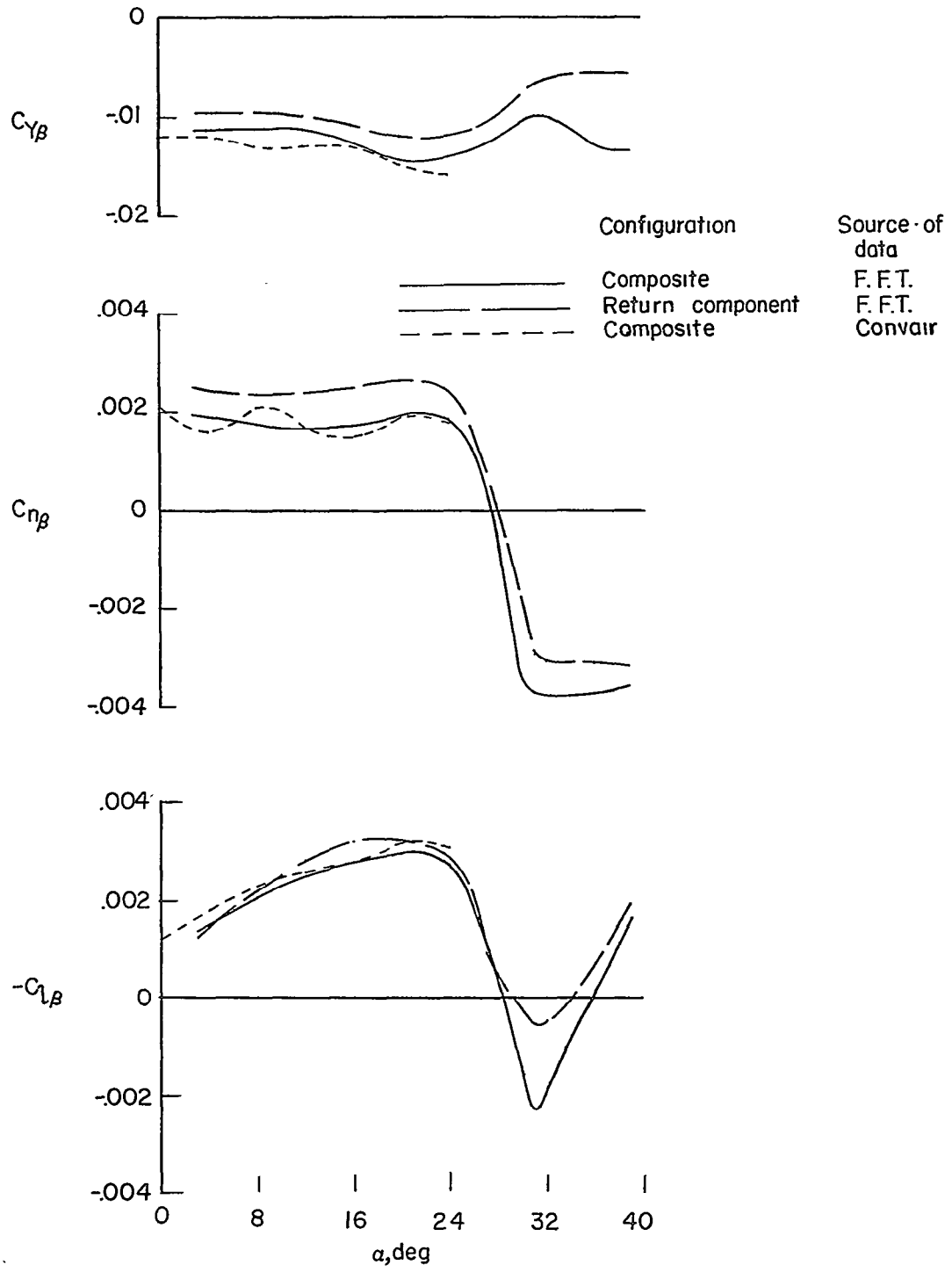

Figure 11.- Comparison of static sideslip characteristics of free-flight models. $\delta_e = 0^\circ$; T = 0 lbs; $\beta = \pm 5^\circ$.

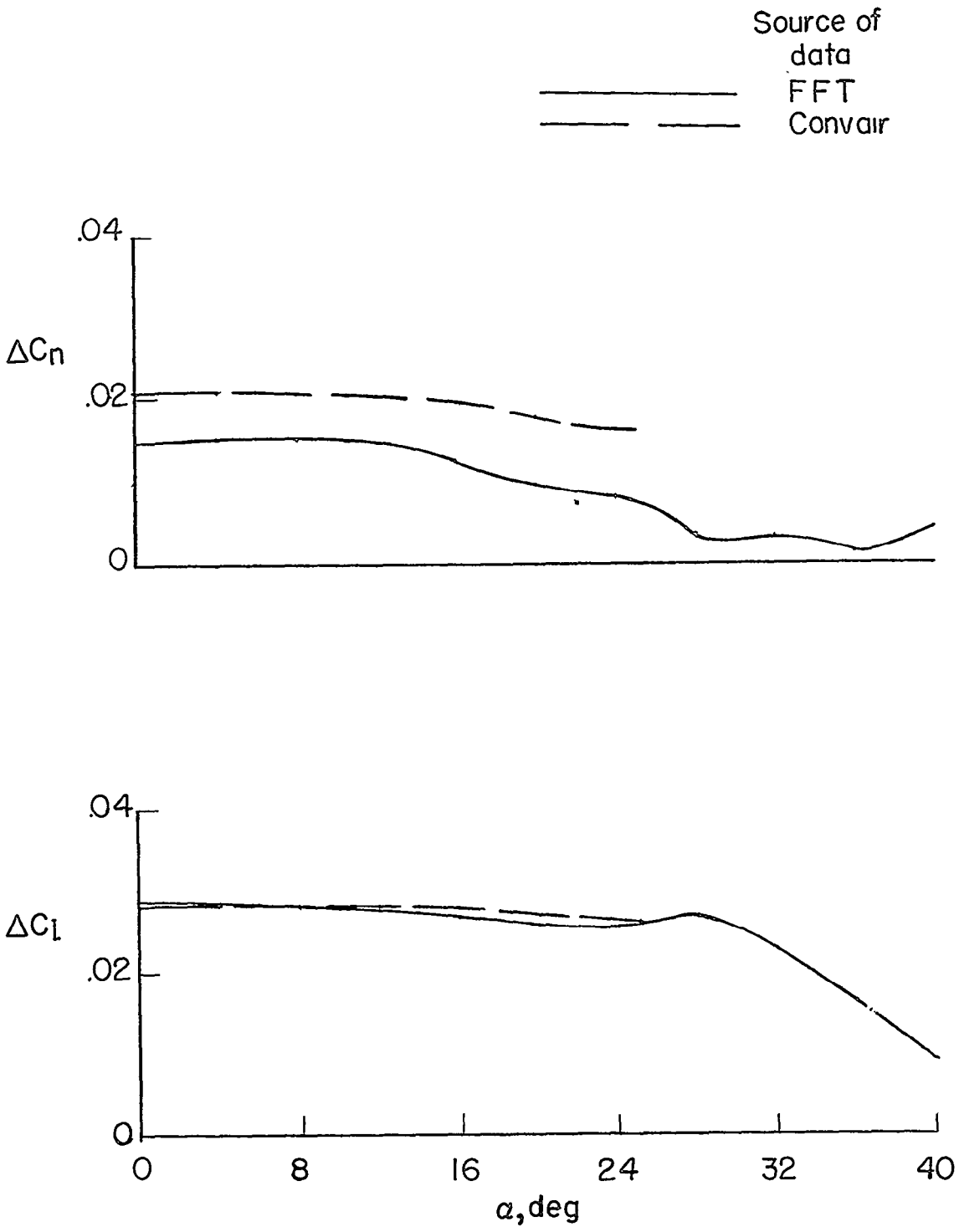

Figure 12.- Comparison of incremental yawing- and rolling-moment coefficients due to aileron deflection of ±15° for the free-flight and Convair return-component models. $\beta = 0^{\circ}$; $\delta_e = 0^{\circ}$.

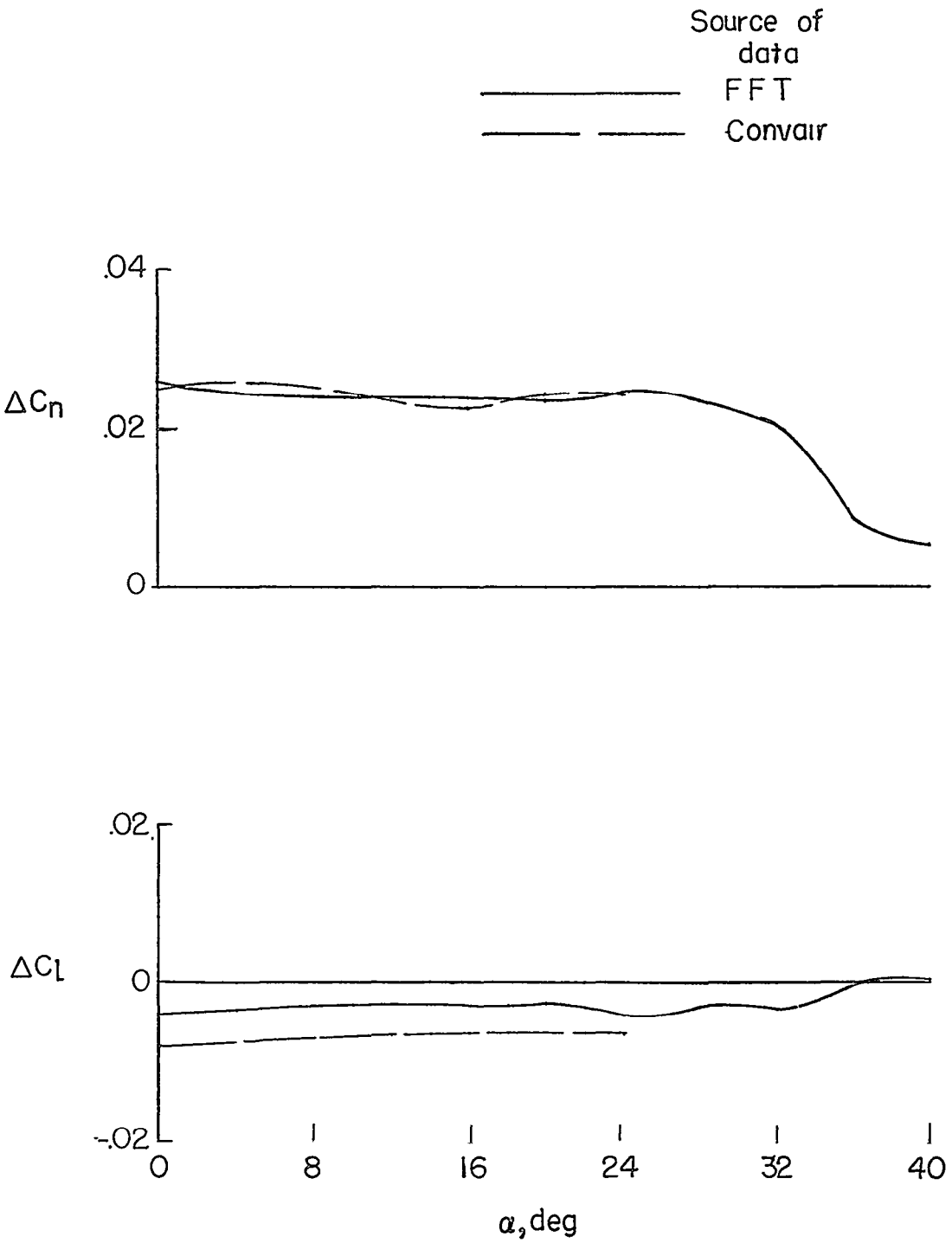

Figure 13.- Comparison of incremental yawing- and rolling-moment coefficients due to rudder deflection of -20° for the free-flight and Convair return-component models. $\beta = 0^{\circ}$; $\delta_e = 0^{\circ}$.

A motion-picture film supplement, carrying the same classification as the report, is available on load. Requests will be filled in the order received. You will be notified of the approximate data scheduled.

The film (16 mm., 9 min., B. and W., silent) deals with an investigation of the low-speed power-on stability and control characteristics of a 1/15-scale free-flying model of the Convair XB-58 airplane. Flights of the composite and return-component configurations were made with and without artificial damping over an angle-of-attack range from 9° to 30°. Flights were also made to determine the effect of dropping the pod.

Requests for the film should be addressed to the

Division of Research Information
National Advisory Committee for Aeronautics
1512 H Street, N. W.
Washington 25, D. C.

NOTE: It will expedite the handling of requests for this classified film if application for the loan is made by the individual to whom this copy of the report was issued. In line with established policy, classified material is sent only to previously designated individuals. Your cooperation in this regard will be appreciated.

[redacted]

CUT

Date_____

Please send, on loan, copy of film supplement to RM SL57K19

_____
Name of organization

_____
Street number

_____
City and State

Attention* Mr._____

Title_____

*To whom copy No.__ of the RM was issued.

INVESTIGATION OF THE LOW-SPEED FLIGHT CHARACTERISTICS OF A 1/15-SCALE MODEL OF THE CONVAIR XB-58 AIRPLANE

COORD. NO. AF-AM-15

By John W. Paulson

ABSTRACT

Flights of the composite and return-component configurations were made with and without artificial damping over an angle-of-attack range from 9° to 30°. Flights were also made to determine the effect of dropping the pod. Static force tests were made at angles of attack from 0° to 40° and over a sideslip range up to ±20°.

INDEX HEADINGS

Stability, Static	1.8.1.1
Stability, Dynamic	1.8.1.2
Control, Longitudinal	1.8.2.1
Control, Lateral	1.8.2.2
Control, Directional	1.8.2.3
Stabilization, Automatic	1.8.8

[redacted]

INVESTIGATION OF THE LOW-SPEED FLIGHT CHARACTERISTICS OF A 1/15-SCALE MODEL OF THE CONVAIR XB-58 AIRPLANE

COORD. NO. AF-AM-15

John W. Paulson

Approved: Thomas A. Harris

Thomas A. Harris
Chief of Stability Research Division
Langley Aeronautical Laboratory

bcc
(10/25/57)

[redacted]